Building Envelope Thermal Activation to Reduce Summer Cooling Peak Demand: It Is All about Holistic Heat Transfer

Preprint

Sajith Wijesuriya,[1] Paulo Cesar Tabares-Velasco,[2] and Marcus V.A. Bianchi[1]

1 National Renewable Energy Laboratory
2 Colorado School of Mines

Presented at the 2022 Buildings XV International Conference
Clearwater Beach, Florida
December 5-8, 2022

NREL is a national laboratory of the U.S. Department of Energy
Office of Energy Efficiency & Renewable Energy
Operated by the Alliance for Sustainable Energy, LLC

This report is available at no cost from the National Renewable Energy Laboratory (NREL) at www.nrel.gov/publications.

Contract No. DE-AC36-08GO28308

Conference Paper
NREL/CP-5500-82638
February 2023

Building Envelope Thermal Activation to Reduce Summer Cooling Peak Demand: It Is All about Holistic Heat Transfer

Preprint

Sajith Wijesuriya,[1] Paulo Cesar Tabares-Velasco,[2] and Marcus V.A. Bianchi[1]

1 National Renewable Energy Laboratory
2 Colorado School of Mines

Suggested Citation
Wijesuriya, Sajith, Paulo Cesar Tabares-Velasco, and Marcus V.A. Bianchi. 2023. *Building Envelope Thermal Activation to Reduce Summer Cooling Peak Demand: It Is All about Holistic Heat Transfer: Preprint*. Golden, CO: National Renewable Energy Laboratory. NREL/CP-5500-82638. https://www.nrel.gov/docs/fy23osti/82638.pdf.

NREL is a national laboratory of the U.S. Department of Energy
Office of Energy Efficiency & Renewable Energy
Operated by the Alliance for Sustainable Energy, LLC

This report is available at no cost from the National Renewable Energy Laboratory (NREL) at www.nrel.gov/publications.

Contract No. DE-AC36-08GO28308

Conference Paper
NREL/CP-5500-82638
February 2023

National Renewable Energy Laboratory
15013 Denver West Parkway
Golden, CO 80401
303-275-3000 • www.nrel.gov

NOTICE

This work was authored in part by the National Renewable Energy Laboratory, operated by Alliance for Sustainable Energy, LLC, for the U.S. Department of Energy (DOE) under Contract No. DE-AC36-08GO28308. Partial funding provided by the U.S. Department of Energy Office of Energy Efficiency and Renewable Energy Building Technologies Office. The views expressed herein do not necessarily represent the views of the DOE or the U.S. Government. The U.S. Government retains and the publisher, by accepting the article for publication, acknowledges that the U.S. Government retains a nonexclusive, paid-up, irrevocable, worldwide license to publish or reproduce the published form of this work, or allow others to do so, for U.S. Government purposes.

Cover Photos by Dennis Schroeder: (clockwise, left to right) NREL 51934, NREL 45897, NREL 42160, NREL 45891, NREL 48097, NREL 46526.

Building Envelope Thermal Activation to Reduce Summer Cooling Peak Demand: It Is All about Holistic Heat Transfer

Sajith Wijesuriya, Ph.D. *Associate Member ASHRAE*
Paulo Cesar Tabares-Velasco, Ph.D.* *Member ASHRAE*
Marcus V.A. Bianchi, Ph.D. *Member ASHRAE*

ABSTRACT

Summer peak electricity demand for cooling in U.S. is anticipated to have an increasing impact on the grid. At the same time, the increased renewable energy generation added to the grid will induce more variability. Grid-interactive efficient buildings are expected to support the electrical grid and provide flexibility as the penetration of renewable energy generation increases. Thermal energy storage can partially provide such support, and, among different technologies, phase change materials (PCMs) embedded in the building envelope can shift space conditioning energy demand away from peak hours. Thermal access to the energy storage on the envelope depends on the heat transfer between the indoor environment and the phase change material in the envelope, which is controlled by the thermal resistances that exist between them. Being able to control such thermal resistances using novel building activation approaches could augment the energy storage potential, determining access to the stored energy. This study numerically analyzes the ability of the combined effect of an optimized PCM in the drywall, thermal resistances, and variable interior heat transfer on their ability to effectively provide flexible response during a time-of-use of three hours in the afternoon using precooling and setback. The analysis particularly considers the peak summer cooling demand in a typical home in Phoenix, AZ. ResStock with EnergyPlus, its simulation engine, is modified to allow for variable heat transfer coefficients and thermal conductivities. Exterior walls, ceiling, and internal mass are individually analyzed with the focus on finding optimal sets of conditions for thermal storage. Preliminary results show that the thermal conductivity of the PCM, natural convection between the envelope and the living space is a "bottle neck" to suppress the PCM performance.

INTRODUCTION

Buildings cooling drives electric peak demand in summer. With increased renewable energy generation added to the grid, and increase in cooling needs, Grid-interactive efficient buildings (GEB) are expected to support the electrical grid and provide flexibility as the penetration of renewable energy generation increases. Within GEB, Thermal Energy Storage (TES) integrated in buildings can shift cooling peak electricity demand [1]. Latent energy storage using phase change materials (PCMs) is popular for passive or active storage. PCMs envelope applications can be macro or microencapsulated. Microencapsulated PCMs are embedded in construction materials like drywall or concrete [2, 3]. However, as a dynamic technology, their benefits depend on several factors such as climate, location within the building, melting temperature as well as its thermal properties [1]. There are efforts to improve envelope performance by: (1) considering a variable thermal conductivity envelope system or reflective roofing system [4-6], (2) developing walls with inner tubes and fins such as heat exchangers [7] that might be inspired by natural flow systems (e.g., rivers) [8, 9]. Some PCM studies show that an increase in thermal conductivity produces faster PCM charging [10-12], while other studies show little improvement on home building energy performance with an increase in drywall thermal conductivity [13], as radiation and convection have an important role in dispatching thermal storage (and affect thermal comfort). In addition, one limitation of PCMs is their static melting temperature, as an optimal PCM for the summer will not perform at all in the winter, and vice-versa [11, 14]. For this reason, some studies examine the possibility of combining different PCMs [15, 16] at a premium. Access to the thermal energy storage in the envelope depends on the heat transfer between the indoor environment and the envelope, which is controlled by the thermal resistances that exist between them: surface heat transfer (convection and radiation) and conduction (thermal conductivity of the layers) resistances. Being able to control such thermal resistances using novel building activation approaches could augment the energy storage potential by, for example, displaying variable thermal resistance of different layers.

Sajith Wijesuriya is a postdoctoral researcher at National Renewable Energy Lab (NREL). **Paulo Cesar Tabares-Velasco** is an ass professor in the Department of Mechanical Engineering, Colorado School of Mines and has a joint appointment at NREL. **Marcus V.A. Bianchi is** a senior researcher at NREL.
*Corresponding author: tabares@mines.edu

Before expensive and time-consuming research is spent on developing new technologies, we propose to numerically quantify the potential and combined effect of an optimized PCM in the drywall, thermal resistances, and variable interior heat transfer on their ability to effectively provide flexible response during different grid events. This study is, therefore, a part of larger project that evaluates the performance of PCMs integrated in building envelopes. Specifically, we use a residential building model implemented in EnergyPlus whole building energy modelling platform to conduct a numerical analysis of the building envelope performance with PCM inclusions under different surface heat transfer conditions and material properties. While PCMs can support winter peak shifting as well, this study looks particularly at the summer peak in Phoenix, AZ to assess the ability of shifting cooling demand.

METHODOLOGY

This study uses EnergyPlus for all calculations employing: (i) principles of heat transfer modelling to simulate PCMs, (ii) ResStock based residential building model for the simulations, (iii) pre-cooling technique implemented with variable surface convection heat transfer coefficients (CHTCs) implemented through an EMS-python plugin, and (iv) a parametric assessment. EnergyPlus has been verified and validated in recent studies in precooling scenarios in homes [17], and to simulate different PCM encapsulation types in the building envelope including microencapsulated PCM embedded in drywall [18, 19]. While the same methodology can be used for materials such as concrete, this study focus on PCMs as most buildings in the US are lightweight buildings that relied on frame construction with drywall (and concrete slab but with a smaller area) as the main thermal storage location within the envelope. PCM/drywall is also easier to retrofit than to replace a frame wall with a concrete wall and has lower embodied energy.

Heat transfer modeling

This study uses the conduction finite difference (CondFD) algorithm that discretizes all opaque envelopes into small spaces between nodes to allow for the linearization of the energy conservation equation that has been previously validated for different types of PCM encapsulations like macroencapsulation and microencapsulation [20, 21]. CondFD discretizes in one-dimension the energy conservation, Equation 1, for node *i* exposed to the indoor environment. The left-hand side of Equation 1 represents the rate of change of the stored energy at each node, while the right-hand equation represents heat fluxes entering and exiting the node.

$$\boldsymbol{\varrho C^A \frac{\Delta x}{2} \frac{T_i^{j+1} - T_i^j}{\Delta t} = k \frac{T_i^j - T_{i+1/2}^j}{\frac{\Delta x}{2}} + h_{surface}^j \left(T_{i+1/2}^j - T_{air}^j \right)}, \qquad (1)$$

Here, ρ is the density of the analyzed element, C^A specific heat term as a function of temperature, k is the thermal conductivity, T is the temperature at time j, $h_{surface}$ is the surface heat transfer coefficient that combines radiation and convection, Δx is the distance between two nodes and Δt is the timestep. Coupling radiation with convection in Equation 1 assumes that the indoor surface temperatures are the same as the indoor air temperature, a common approximation for insulated exterior walls [22].

Analyzed residential building

Figure 1 shows a typical home built in the 2000s in Arizona and is developed using ResStock building stock which is a free, open-source building simulation tool [23]. ResStock combines multiple public and private data to construct probabilistic distributions of more than 100 physical and operational characteristics of single-family homes, then statistically samples from those collections to generate 350,000 EnergyPlus models of statistically representative homes across the USA. We have extracted a ResStock developed EnergyPlus input data file (idf) and modified it to allow for variable properties and surface characteristics using EnergyPlus version 22.1.0 released in 2022 as suggested by [24]. This single-family home model uses thermophysical properties and building characteristics obtained from IECC 2009 standards, Residential Energy Consumption Survey (RECS) 2009, National Association of Home Builders (NAHB), Residential Building Stock Assessment (RBSA) 2012, American Community Survey (ACS) and several other key publications as listed in [25].

The home comprises a living zone and a garage zone. It is simulated with two thermal zones: the conditioned living zone and the garage. The conditioned living zone has an area of 185.8 m^2 (2,000 ft^2) and (a) six exterior wall surfaces, (b) two interior interzonal wall surfaces which are shared with the garage zone, (c) floor surface, (d) ceiling surface, (e) living space partitions.

Exterior walls have one side exposed to the ambient environment. Interior interzonal walls have one side exposed to an unconditioned zone (in this case, garage). For this study, PCMs are assumed to be mixed in the drywall of exterior walls, internal walls, and ceiling. Each potential PCM location is analyzed separately to evaluate their impact on the heat transfer behavior and the energy needs of the building. All three of these surface types include drywall as the interior layer, which serves as a substrate for the infusion of PCMs. Table 1 shows the layer structure of each envelope. Ground thermal coupling is modeled through the foundation Kiva model included in EnergyPlus. Kiva is a comprehensive 3D foundation heat transfer calculation tool, previously verified [26]. Home is simulated using the TMY3 weather for Phoenix, Arizona.

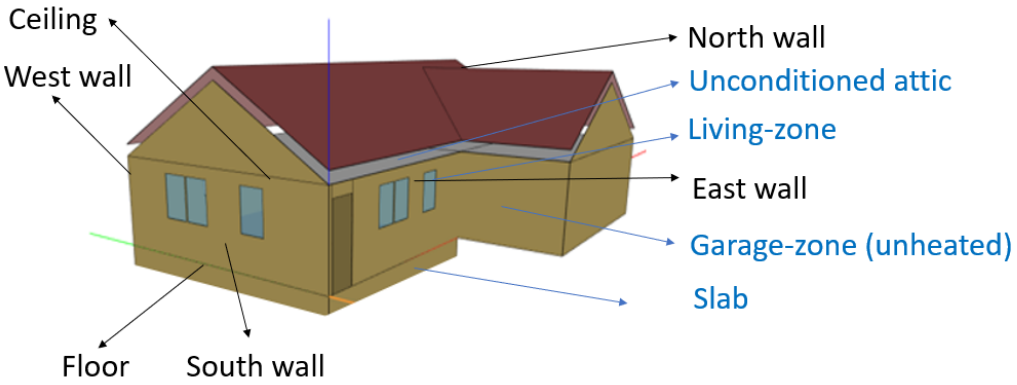

Figure 1. Analyzed single family residential building.

This study assumes that microencapsulated PCM is imbedded in the drywall, representing 20% of total weight. The PCM has a melting temperature range of 22.5-24.7°C (72.5-76.5°F) and latent heat of 23 J/g (9.9 Btu/lb) as 20% of the weight in the drywall is PCMs. These values were obtained from a previous parametric assessment conducted by [27]. The baseline case considers a drywall thermal conductivity of 0.15 W/m-K (0.087 Btu/(h·ft·°F)) [1, 28]. PCM drywall is only implemented in the ceiling, exterior walls, and internal walls. The specific heat capacity contributions from each material are shown for these envelope types in Table 1. Note that the specific heat capacity for PCM drywall is indicated during the phase change. Specific heat capacity of the drywall increases by ~15 times during phase change. The thermal, solar, and visible absorptance values for the asphalt shingles are 0.91, 0.85, 0.85, respectively. Space conditioning of the house is provided by a residential air source heat pump.

Table 1. Layer structure of the envelopes

Envelope	Layer structure (Exterior to interior)	Thermal Resistance $ft^2 \cdot °F \cdot h/BTU$ ($m^2 \cdot K/W$)	Specific heat capacity: kJ/kg/K (BTU/lb/°F)
Roofing	Asphalt shingles, Roof Sheathing, Insulation	0.3 (1.7)	-
Ceiling	Insulation, Drywall	38.0 (6.7)	Insulation = 1.1 (0.3), Drywall = 0.8 (0.2) PCM drywall = 11.9 (2.8)*
Exterior wall	Vinyl siding Wall sheathing Wall stud and cavity insulation, Drywall	10.1 (1.8)	Vinyl coating =1.0 (0.2), Wall sheathing = 1.2 (0.3) Wall stud and cavity insulation = 1.2 (0.3) Drywall = 0.8 (0.2), PCM drywall = 11.9 (2.8)*
Floor	On grade concrete slab, Floor carpet	2.1 (0.4)	Concrete slab = 0.8 (0.2)
Internal wall	Wall sheathing, Wall stud and cavity, Drywall	8.9 (1.6)	Wall sheathing = 1.2 (0.3), Wall stud and cavity =1.2 (0.3), Drywall = 0.8 (0.2) PCM drywall= 11.9 (2.8)*

*Within the phase change interval of 22.5 - 24.7°C (72.5-76.5 °F)

Table 2. HVAC system information

System component	Property	Value
Heat pump (Cooling mode)	Rated COP	4.1
	Gross rated cooling capacity	21.3 kW (72.7 kBtu/h)
Heat pump (Heating mode)	Rated COP	3.3
	Gross rated heating capacity	21.3 kW (72.7 kBtu/h)
Supplementary heating coil	Fuel	Electric
	Nominal capacity	6.3 kW (21.5 kBtu/h)

Precooling strategy with variable surface heat transfer coefficients

This study uses a cooling setpoint schedule based on a previous optimization study which found that a similar home in Phoenix requires at least 5 hours of precooling [29-31]. The peak time for the evaluated location is from 3 p.m. – 6 p.m. as defined by the Salt-River Project utility time-of-use rates in Phoenix, Arizona. Therefore, the pre-cooling time is from 10 a.m. – 3 p.m. As shown in Figure 2a, the red-shaded range indicates peak hours, while the blue-shaded range shows the pre-cooling period. We also replaced the baseline convection values with variable values during precooling and setback times as shown in Figure 2b (h values are shown in W/m^2-K in the figure legend).

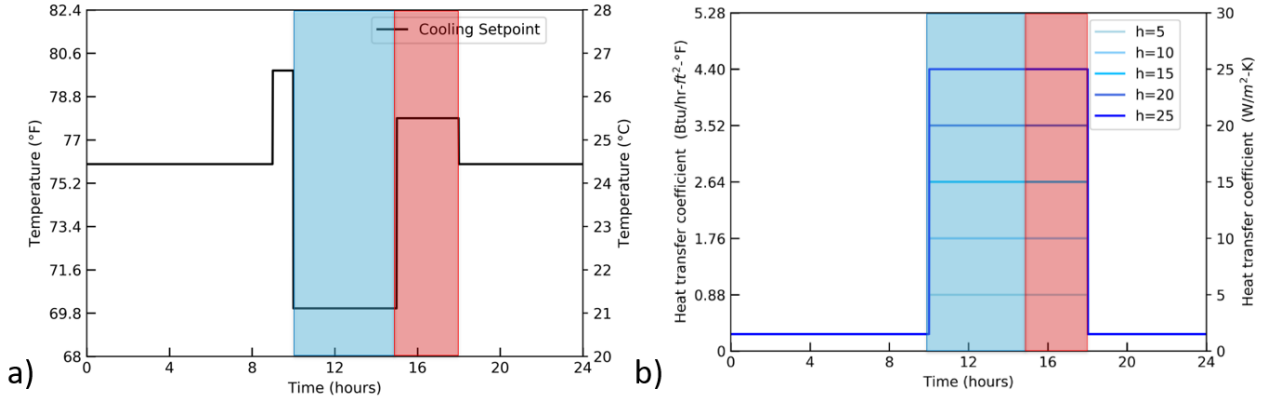

Figure 2. Variable setpoint strategy with a) 21.1 °C (70°F) pre-cooling temperature from 10 a.m. to 3 p.m. and 25.6°C (78°F) setback temperature from 3 p.m. to 6 p.m. and b) variable surface heat transfer coefficients that are increased only during precooling and setback times.

We implemented variable surface CHTCs in the selected surfaces (exterior wall, internal wall, or ceiling) inside the living space operating during the entire period of precooling and setback hours (from 10 a.m. to 6 p.m.). Although EnergyPlus has a natural and forced convection models (TARP and CeilingDiffuser) [32], these are bypassed and replaced with a constant value schedule that increases the heat transfer coefficient from 10 a.m. to 6 p.m. and switches the model back to use typical natural convection coefficients for indoor environment as calculated by TARP model: 1.5 W/m^2-K (0.26 Btu/(h·ft·°F)) for the rest of the day as shown in Figure 2b. This switching of CHTCs is implemented using an EnergyPlus Energy Management System (EMS) python plugin. Previous literature shows interior CHTCs as high as ~12 W/m^{2}K (2.1 Btu/(h·ft·°F)) next to a mechanical flow device [33]. To investigate the theoretical impact of high CHTCs we simulated values up to 25 W/m^2-K (4.4 Btu/(h·ft·°F)). We also assumed that in an actual setting, a mechanical air flow device like a fan would be used to increase the CHTC [34].

The thermal conductivity of organic PCMs typically used in building applications varies in the 0.1 – 0.5 W/m-K (0.058 – 0.29 Btu/(h·ft·°F)) range. Salt hydrates have conductivity in the range of 0.2 – 1.5 W/m-K (0.12 – 0.87 Btu/(h·ft·°F)) [35, 36]. Therefore, we assumed the thermal conductivity of PCM infused drywall to ranging between 0.25 – 2.0 W/m-K (0.14 – 1.15 Btu/(h·ft·°F)). Parametric analysis was then conducted with five heat transfer coefficient values, five PCM drywall thermal conductivity values, and three locations of PCM inclusion in drywall. Each envelope component (exterior wall, internal wall, and ceiling) is activated independently to assess their respective impact adding up to 75 simulations. Results for a single day (July 2nd) for the south facing exterior wall are presented in the following section.

RESULTS

Figure 3a shows the cooling setpoint (CSP) and predicted indoor air temperature variation of the living zone for July 2nd when PCM is present (and activated) in exterior wall (Figure 4a), ceiling (Figure 4b) and internal wall (Figure 4c) with different convection coefficients 1.5 (baseline) to 25 W/m^{2}K. During this sunny and clear day, the outside air temperature ranged from 31.7°C (89.1°F) to 42.8°C (109.0°F), representative of a hot summer day. A single day is selected to facilitate qualitative comparison between different transfer rates and all figures are zoomed from 8 a.m. – 8 p.m. since the surface heat transfer coefficients are varied only between 10 a.m. and 6 p.m. The "baseline" case does not include PCMs and uses a regular Drywall layer with a thermal conductivity of 0.15 W/m-K (0.087 Btu/h-ft-°F) and a CHTC of 1.5 W/m^2-K (0.26 Btu/(h·ft^2·°F)) at the interior side of all envelopes, with the same cooling setpoint schedule.

For PCM cases, only the CHTC is varied from 5 W/m^2-K to 25 W/m^2-K (0.88 to 4.4 Btu/(h·ft^2·°F)) in increments of 5 W/m^2-K (0.88 Btu/(h·ft^2·°F)). Cooling setpoint (CSP) is also shown in each figure for reference. PCM is only included in either exterior wall, ceiling, or internal walls. Surface heat transfer coefficient is only increased on the surfaces with the PCM inclusions. CHTC on the remaining surfaces in the living zone is kept at 1.5 W/m^2-K (0.26 Btu/(h·ft^2·°F)) if only a specific surface got activated for higher convective heat transfer. The low surface CHTC of the baseline case has a weak coupling with the envelope and therefore, surface wall temperature quickly cools down and warms up compared to all cases. PCM and the CHTC (h) delay the indoor air temperature meeting the setpoint when compared with the baseline case. The least impact is shown by the internal walls. Figure 3b shows that having PCMs with surface CHTC of 10 W/m^2-K (1.76 Btu/(h·ft^2·°F)) or above on the ceiling delays the temperature increase during the setback for entire peak time. Exterior walls show an impact between the other two envelope types.

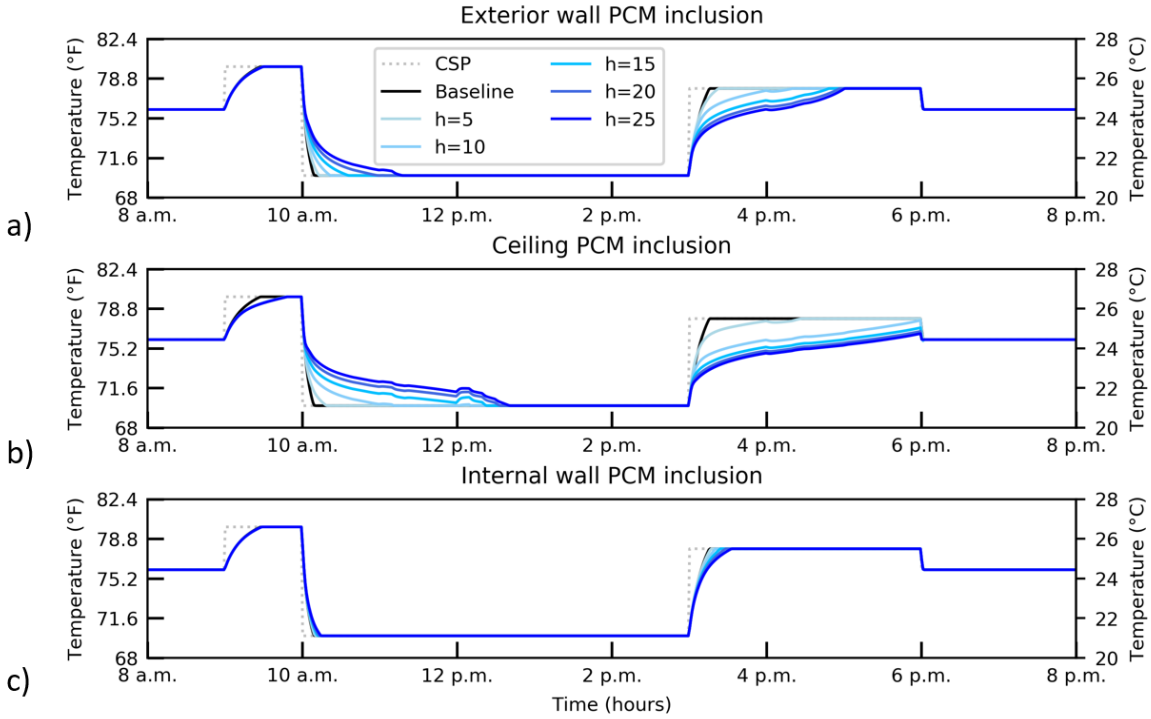

Figure 3. Cooling setpoint (CSP) and predicted living zone mean air temperature from 8 a.m. – 8 p.m. on July 2nd for home with variable surface heat transfer coefficients (1.5 or baseline to 25 W/m^{2}K) and PCMs in the: a) exterior wall only, b) ceiling only, and (c) internal walls only.

Figure 4 shows the impact that surface heat transfer coefficients (a, c, d) and drywall thermal conductivity (b, d, f) has on melted fraction of exterior wall (a, b), ceiling (c, d) and internal wall (e, f) PCM. For the plots with varying h, the k value of the PCM drywall for all cases is 0.25 W/m-K (0.14 Btu/h-ft-°F). For the plots with varying k, the h value at the PCM drywall for all cases is 5 W/m^2-K (0.88 Btu/h-ft^2-°F). Surface heat transfer has a stronger effect than thermal conductivity to increase

the effective use of PCM; CHTC of 20 W/m^2-K (3.52 Btu/h-ft^2-°F) is needed for this PCM to fully freeze/charge in all envelope types. In fact, with higher surface heat transfer coefficients, precooling period could be shortened by 1-2 hours as higher surface heat transfer accelerates heat transfer to the PCMs and completely freeze PCMs in about 2-3 hours. Furthermore, increasing the CHTC and thermal conductivity both show diminishing returns at higher values. Exterior wall and ceiling show similar charging behavior as heat is lost to the living zone. The discharging nature is different between all the locations within the envelope as the heat must come through the resistance of the insulation to melt the PCM, which is shown by slow discharge of the ceiling. Both Figure 4b and Figure 3b indicate that for this home and weather, having PCMs in the ceiling is most effective approach. Comparing melted fractions in Figure 4 for cases varying CHTC vs varying thermal conductivity shows natural convection between the envelope and the living space is a "bottle neck" to suppress the PCM performance than the thermal conductivity of the PCM.

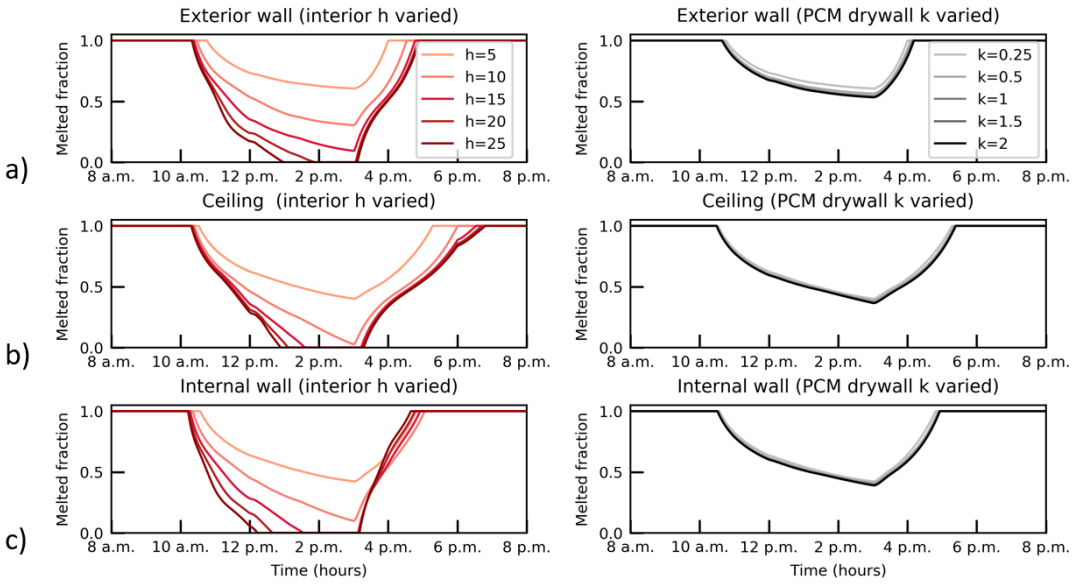

Figure 4. Melted fraction of the PCM in the drywall from 8 a.m. – 8 p.m. on July 2nd for home with: PCMs in exterior south facing wall with a) variable CHTC and b) different constant values of thermal conductivity; ceiling with c) variable CHTC and d) different constant values of thermal conductivity; and internal wall with e) variable CHTC and f) different constant values of thermal conductivity.

Figure 5 shows net heat flux for the three analyzed surfaces with variable surface heat transfer coefficients. The thermal conductivity of the PCM drywall for all cases is 0.25 W/m-K (0.14 Btu/h-ft-°F). The net heat flux is the sum of the heat flux entering/leaving each side of the PCM-drywall. Positive values indicate the net heat flux direction is into the living zone (cooling or charging the PCM), negative values indicate net heat flux is leaving the living zone (heating or discharging the PCMs). The wavy behavior of the heat flux curves is driven by other heat gains schedules of the building like internal gains, and infiltration.

When the surface heat transfer coefficient increases from 5 to 25 W/m^2-K (0.88 to 4.4 Btu/(h·ft^2·°F)), peak heat transfer of charging increases by 2.56 kJ/m^2 (0.23 Btu/ft^2) for the exterior wall, by 1.62 kJ/m^2 (0.14 Btu/ft^2) for the ceiling, and 1.76 kJ/m^2 (0.15 Btu/ft^2) for the internal wall. High heat loss through the exterior wall is influenced by the exterior heat flux as well and therefore, exterior wall takes the longest time to freeze the PCM. Moreover, under same conditions discharge heat transfer increases by 2.38 kJ/m^2 (0.21 Btu/ft^2) for the exterior wall, 0.9 kJ/m^2 (0.08 Btu/ft^2) for the ceiling, and 1.7 kJ/m^2 (0.15 Btu/ft^2) for the internal wall. Here the exterior wall discharges (melts PCM) quickest supported again by the heat flux from exterior. Ceiling shows slow melting and can hold its charge for a longer time than both the internal wall and the exterior wall.

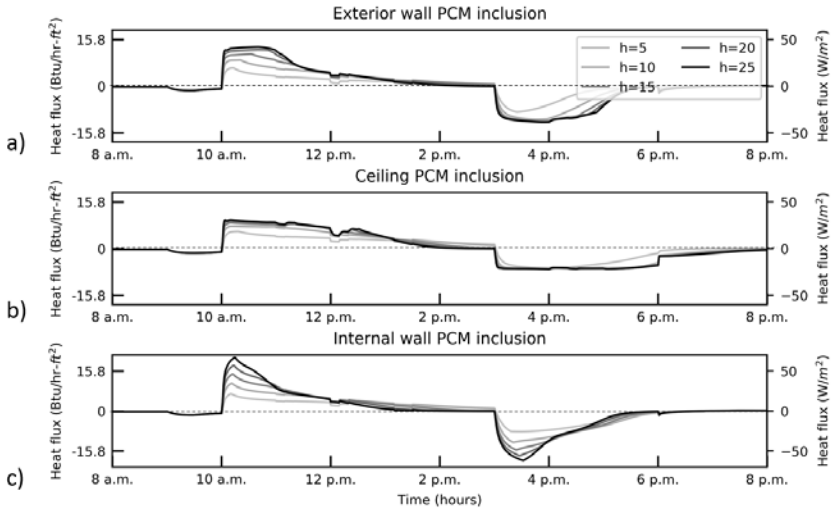

Figure 5. Net heat flux at the PCM drywall layer from 8 a.m. – 8 p.m. on the second day of July for (a) exterior wall only, (b) ceiling only, (c) internal walls only. Positive value represents charging and negative values represent discharging.

Figure 6 shows the impact zthe variable CHTCs have on different exterior wall orientations (South, North, East, and West) for surface coefficients of 5, 15, and 25 W/m^2-K (0.88, 2.6, and 4.4 Btu/(h·ft^2·°F)) respectively. The thermal conductivity of the PCM drywall for all cases remain 0.25 W/m-K (0.14 Btu/h-ft-°F). East wall has the slower precooling response/ charging due to morning solar exposure that translates to lower net heat transfer rates. These differences reduce substantially when heat transfer coefficient values are 15 W/m^2-K (2.64 Btu/h-ft^2-°F) or higher. These separations are not visible during the discharging of the PCMs at high CHTC values since the heat transfer from outside towards inside supports the PCM melting.

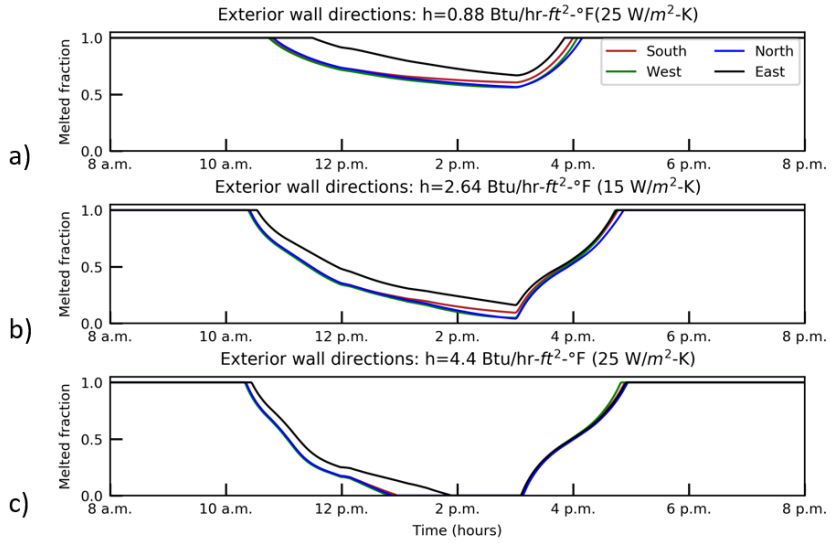

Figure 6. Melted fraction of the PCM in the drywall of the exterior wall from 8 a.m. – 8 p.m. on July 2nd. PCMs are implemented in exterior walls only. Each line represents wall orientations (South, North, East, and West) when surface CHTCs are increased from baseline value to a) 5 (0.88 Btu/h-ft^2-°F), b) 15 (2.6 Btu/h-ft^2-°F) and c) 25 W/m^2-K (4.4 Btu/h-ft^2-°F). Charging time is from 10 a.m. to 3 p.m., and peak time is from 3 p.m. to 6 p.m.

Finally, **Figure 7** shows the impact variable surface heat transfer coefficients have on cooling electric rate of the house on the selected day. The thermal conductivity of the PCM drywall for all cases remain 0.25 W/m-K (0.14 Btu/h-ft-°F). Having PCMs in the ceiling with high surface heat transfer coefficients fully shifts the peak cooling electricity demand when the CHTCs 10 W/m^2-K (1.76 Btu/(h·ft^2·°F)) or above. Although, PCM drywall in exterior wall and internal wall cannot fully shift

the peak but increasing the PCM percentage can potentially completely shift the peak cooling demand.

PCMs and the increased heat transfer coefficients further increase the cooling electricity rate now that additional cooling is transferred to the PCM infused drywall layer to charge/freeze the PCM. However, due to both precooling, PCMs, and the heat transfer condition, the cooling rate during the peak time is significantly decreased. For an instance, when the PCM is included in the ceiling, and CHTC is 10 W/m^2-K (1.76 Btu/(h·ft^2·°F)) the cooling electricity use increases by 23.9 % during charging and the cooling electricity consumption during peak hours decreases by 100% (fully shifting the peak). Considering the same case, during the week considered, total energy consumption increases by 2.1% but fully shifts peak cooling energy for all 7 days. The removal of cooling electricity use from peak time would lead to reduced stress on the electricity grid, and potentially reduce electricity costs to the consumer when the Time of Use (ToU) rates are applied.

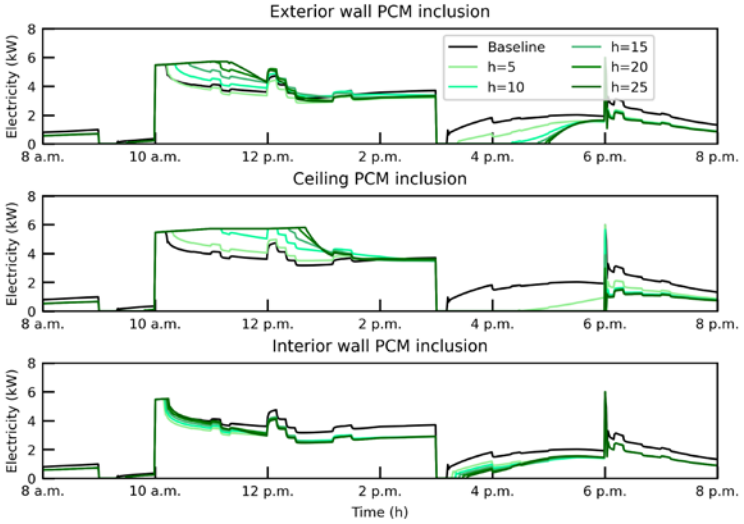

Figure 7. Cooling electricity demand of the building from 8 a.m. – 8 p.m. on the second day of July. PCMs are implemented in the (a) exterior wall only, (b) ceiling only, (c) internal walls only. Charging time is from 10 a.m. to 3 p.m., and peak time is from 3 p.m. to 6 p.m.

CONCLUSIONS

This study conducts a parametric assessment to evaluate the impact of PCM thermal conductivity and interior surface convective transfer on the thermal and energy performance of a home located in Phoenix, AZ during Summer. Cooling electricity demand peak is identified based on Time-of-Use electricity rates used by Salt-River project utility. Exterior wall, ceiling, and internal wall envelopes are investigated to find the ability to shift the peak cooling demand when parameter values are varied while using a suitable pre-cooling strategy by operating the cooling HVAC. For the analyzed house, based on the ability to shift the peak cooling electricity demand, the ceiling surface offers the most beneficial PCM inclusion as far as the location is considered, followed by exterior wall, and internal wall shared with an unconditioned garage zone.

Results also show that the PCM use is greatly impacted by the variation of the CHTC when compared with the thermal conductivity of the PCM drywall because convection between the envelope and the living space is a “bottle neck” to suppress or augment heat transfer between the PCM and indoor environment. Even if the thermal conductivity of the PCM drywall is increased by 8x very little benefit is observed. When increasing the CHTC by 4x, all investigated envelopes show complete phase change of the PCM. Results also show that cooling electricity consumption during peak hours is shifted by 100% at a CHTC of 10 W/m^2-K (0.88 Btu/(h·ft^2·°F)) and a PCM drywall thermal conductivity of 0.25 W/m-K (1.73 Btu/h-ft-°F) just by using PCMs in the ceiling. This would contribute to relieve the stress on the electricity grid during the summer and facilitate to utilization of the off-peak, surplus renewable energy generation in the grid. While this study only considers one home in a hot-dry weather, similar strategies can be used for winter weather with a suitable PCM and a preheating strategy. Within the scope of this study, the results indicate the need for increasing the CHTC value rather than increasing the thermal conductivity value of the PCM. Experiments-based studies are needed to further confirm these conclusions. The actual outcomes would depend on the maximum heat transfer coefficients achieved next to the internal wall surfaces without compromising the user comfort.

NOMENCLATURE

Δx	=	Spatial discretization
Δt	=	Timestep
ρ	=	Density
ACS	=	American Community Survey
ASHARE	=	American Society of Heating Air-conditioning and Refrigeration Engineers
CondFD	=	Conduction finite different
CHTC	=	Convection Heat Transfer Coefficient
$h_{surface}$	=	Heat transfer coefficient next to the surface
idf	=	Input data file
IECC	=	International Energy Conservation Code
NAHB	=	National Association of Home Builders
PCM	=	Phase change material
RBSA	=	Residential Building Stock Assessment
RECS	=	Residential Energy Consumption Survey
ResStock	=	Residential building analysis tool
T	=	Temperature
TES	=	Thermal energy storage

Subscripts

air	=	Air node
surface	=	Building envelope surface
i	=	i^{th} node
j	=	j^{th} time

REFERENCES

1. Wijesuriya, S., M. Brandt, and P.C. Tabares-Velasco, *Parametric analysis of a residential building with phase change material (PCM)-enhanced drywall, precooling, and variable electric rates in a hot and dry climate.* Applied Energy, 2018. **222**: p. 497-514.
2. Mazzucco, G., et al., *Modeling Techniques of Storage Modules with PCM Microcapsules: Case Study.* Journal of Energy Engineering, 2017. **144**(1): p. 05017005.
3. Nghana, B. and F. Tariku, *Phase change material's (PCM) impacts on the energy performance and thermal comfort of buildings in a mild climate.* Building and Environment, 2016. **99**: p. 221-238.
4. Shekar, V. and M. Krarti, *Control strategies for dynamic insulation materials applied to commercial buildings.* Energy and Buildings, 2017. **154**(Supplement C): p. 305-320.
5. Park, B., W.V. Srubar, and M. Krarti, *Energy performance analysis of variable thermal resistance envelopes in residential buildings.* Energy and Buildings, 2015. **103**(Supplement C): p. 317-325.
6. Park, B. and M. Krarti, *Energy performance analysis of variable reflectivity envelope systems for commercial buildings.* Energy and Buildings, 2016. **124**(Supplement C): p. 88-98.
7. Craig, S. and J. Grinham, *Breathing walls: The design of porous materials for heat exchange and decentralized ventilation.* Energy and Buildings, 2017. **149**(Supplement C): p. 246-259.
8. Bejan, A. and S. Lorente, *The constructal law and the evolution of design in nature.* Physics of Life Reviews, 2011. **8**(3): p. 209-240.
9. Bejan, A. and S. Lorente, *The constructal law and the thermodynamics of flow systems with configuration.* International Journal of Heat and Mass Transfer, 2004. **47**(14): p. 3203-3214.
10. Biswas, K., P. Childs, and A. J, *Testing of Nano-PCM-Enhanced Building Envelope Components in a Warm-Humid Climate*. 2013, Oak Ridge National Laboratory: Oak Ridge

11. Kalnæs, S.E. and B.P. Jelle, *Phase change materials and products for building applications: A state-of-the-art review and future research opportunities.* Energy and Buildings, 2015. **94**: p. 150-176.
12. Saeed, R.M., et al., *Preparation and enhanced thermal performance of novel (solid to gel) form-stable eutectic PCM modified by nano-graphene platelets.* Journal of Energy Storage, 2018. **15**: p. 91-102.
13. Brandt, M., S. Wijesuriya, and P.C. Tabares-Velasco, *Optimization of PCM-Enhanced Drywall Installed in Walls and Ceilings for Light-Weight Residential Buildings*, in *10th Conference on Advanced Building Skins*. 2015: Bern, Switzerland. p. 10.
14. Ascione, F., et al., *Energy refurbishment of existing buildings through the use of phase change materials: Energy savings and indoor comfort in the cooling season.* Applied Energy, 2014. **113**(Supplement C): p. 990-1007.
15. Jin, X. and X. Zhang, *Thermal analysis of a double layer phase change material floor.* Applied Thermal Engineering, 2011. **31**(10): p. 1576-1581.
16. Pasupathy, A. and R. Velraj, *Effect of double layer phase change material in building roof for year round thermal management.* Energy and Buildings, 2008. **40**(3): p. 193-203.
17. Booten, C. and P.C. Tabares-Velasco. *Using EnergyPlus to Simulate the Dynamic Response of a Residential Building to Advanced Cooling Strategies*. in *The Second International Conference on Building Energy and Environment,*. 2012. Boulder, CO.
18. Tabares-Velasco, P.C., et al., *Verification and validation of EnergyPlus phase change material model for opaque wall assemblies.* 2012. **54**: p. 186-196.
19. Wijesuriya, S., et al., *Empirical validation and comparison of PCM modeling algorithms commonly used in building energy and hygrothermal software.* 2020. **173**: p. 106750.
20. Wijesuriya, S., et al., *Empirical validation and comparison of PCM modeling algorithms commonly used in building energy and hygrothermal software.* Building and Environment, 2020. **173**: p. 106750.
21. Tabares-Velasco, P.C., C. Christensen, and M. Bianchi, *Verification and validation of EnergyPlus phase change material model for opaque wall assemblies.* Building and Environment, 2012. **54**(0): p. 186-196.
22. Mitchell, J.W. and J.E. Braun, *Principles of Heating, Ventilation, and Air Conditioning in Buildings.* 2013, Hoboken: Wiley.
23. Wilson, E.J., *ResStock-Targeting Energy and Cost Savings for US Homes*. 2017, National Renewable Energy Lab.(NREL), Golden, CO (United States).
24. Tabares-Velasco, P.C. and B. Griffith, *Diagnostic test cases for verifying surface heat transfer algorithms and boundary conditions in building energy simulation programs.* Journal of Building Performance Simulation, 2012. **5**(5): p. 329-346.
25. Wilson, E.J., et al., *Energy Efficiency Potential in the U.S. Single-Family Housing Stock*. 2017: United States. p. Medium: ED; Size: 157 p.
26. Kruis, N. and M.J.J.o.B.P.S. Krarti, *KivaTM: a numerical framework for improving foundation heat transfer calculations.* 2015. **8**(6): p. 449-468.
27. Wijesuriya, S., M. Brandt, and P.C.J.A.e. Tabares-Velasco, *Parametric analysis of a residential building with phase change material (PCM)-enhanced drywall, precooling, and variable electric rates in a hot and dry climate.* 2018. **222**: p. 497-514.
28. Darkwa, K., P. O'Callaghan, and D.J.A.E. Tetlow, *Phase-change drywalls in a passive-solar building.* 2006. **83**(5): p. 425-435.
29. Turner, W.J.N., I.S. Walker, and J. Roux, *Peak load reductions: Electric load shifting with mechanical pre-cooling of residential buildings with low thermal mass.* Energy, 2015. **82**: p. 1057-1067.
30. Brandt, M., S. Wijesuriya, and P.C. Tabares-Velasco, *Optimization of PCM-Enhanced Drywall Installed in Walls and Ceilings for Light-Weight Residential Buildings*. 2015: Golden, CO.
31. Arababadi, R. and K. Parrish, *Modeling and testing multiple precooling strategies in three residential building types in the Phoenix climate*, in *2016 ASHRAE Annual Conference*. 2016, ASHRAE: St. Louis, MO. p. 202-214.
32. Liu, J., et al., *The impact of surface convective heat transfer coefficients on the simulated building energy consumption and surface temperatures.* 2014.
33. Khalifa, A.-J.N., R.J.I.J.o.H. Marshall, and M. Transfer, *Validation of heat transfer coefficients on interior building surfaces using a real-sized indoor test cell.* 1990. **33**(10): p. 2219-2236.
34. Kosky, P., et al., *Exploring engineering: an introduction to engineering and design*. 2015: Academic Press.
35. Abhat, A.J.S.e., *Low temperature latent heat thermal energy storage: heat storage materials.* 1983. **30**(4): p. 313-332.
36. Cabeza, L.F., et al., *Materials used as PCM in thermal energy storage in buildings: A review.* 2011. **15**(3): p. 1675-1695.